Icarus 297 (2017) 110–118

Contents lists available at ScienceDirect

Icarus

journal homepage: www.elsevier.com/locate/icarus

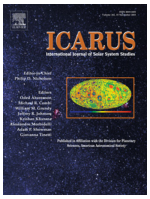

# Direct detection of gaps in Saturn's A ring

Morgan E. Rehnberg*, Zarah L. Brown, Larry W. Esposito, Nicole Albers

*Laboratory for Atmospheric and Space Physics, University of Colorado, 3665 Discovery Drive, Boulder, CO 80303-7820, United States*

ARTICLE INFO

*Article history:*
Received 26 October 2016
Revised 10 May 2017
Accepted 27 June 2017
Available online 28 June 2017

*Keywords:*
Planetary rings
Saturn
Rings

ABSTRACT

Indirect observations spanning decades have indicated that Saturn's A ring is populated with a plethora of self-gravity wakes, small wavelike structures that arise from the gravitational attraction between ring particles. We present the direct detection of the gaps that represent the minima between the denser wakes. Through a statistical test, we analyze a series of seven high-resolution stellar occultations observed by the *Cassini* Ultraviolet Imaging Spectrograph to identify nearly half a million discrete regions with an optical depth less than a quarter of the surrounding ring. These gaps correlate strongly with previous observations of the A-ring brightness asymmetry.

## 1. Introduction

Evidence that Saturn's rings are structurally inhomogeneous on small scales predates the *Cassini* mission. Ground-based observations revealed that the main rings were brighter at their ansae (the locations of greatest observed radial extent) than at the sub-observer point (Ferrin, 1975; Price and Baker, 1975; Lumme et al., 1977; French et al., 2007). Detailed analyses of *Voyager* images by Dones et al. (1993) demonstrated that such a brightness asymmetry is not an effect of Earth-based observation. Since the arrival of *Cassini*, observations by the Ultraviolet Imaging Spectrograph (Colwell et al., 2006; 2007), Visual and Infrared Mapping Spectrometer (Hedman et al., 2007; Nicholson and Hedman, 2010), and Composite Infrared Spectrometer (Ferrari et al., 2009) have provided confirmation across a broad range of wavelengths.

Toomre (1964) provided early theory describing instabilities in particle disks, even without the presence of an external perturber. Colombo et al. (1976) and Franklin and Colombo (1978) showed that Saturn's brightness asymmetry could be produced by series of such aligned particle wakes. Theory and simulations indicate that such structures coalesce through self-gravitation and are sheared by differential Keplerian rotation (Salo, 1995; Salo et al., 2004). Simplified, infinitely-long "granola bar" models of these wakes have been shown to reproduce the varying brightness observed in occultations by UVIS and VIMS, but this remains indirect evidence for the presence of self-gravity wakes in Saturn's A ring (Colwell et al., 2006; Hedman et al., 2007). This work presents the direct detection of these wakes, namely the gaps that represent the features' minima.

## 2. Data

This study uses stellar occultations observed by the High Speed Photometer (HSP) of the *Cassini* Ultraviolet Imaging Spectrograph (UVIS), described in detail by Esposito et al. (2004). A discrete optical train within the spectrograph, HSP measures flux from a target star on a rapid cadence, 500 or 1000 Hz for the observations used in this work.

### 2.1. Optical depth and geometric solution

The target star's flux $I_0$ is attenuated by any material between the star and the instrument. We assume that all such attenuation is the result of material in Saturn's rings. For a region of the rings with line-of-sight optical depth $\tau$, the flux reaching HSP is $I = I_0 e^{-\tau} + b$, where $b$ is the background of ancillary light entering the aperture of the photometer. The instrument measures $I\Delta t$ for each sampling period $\Delta t$. Although, in an ideal situation, $I_0$ would remain constant for the duration of the observation (ignoring stellar variability), HSP actually becomes more sensitive as an observation progresses (Colwell et al., 2007). To account for this "ramping up," we use a variable $I_0$ measured in unocculted regions and interpolated elsewhere. The background $b$ is conversely measured at locations of complete attenuation.

We can rearrange the above formula and account for the spacecraft's angle of elevation with respect to the rings $B$ to derive an expression for the normal optical depth $\tau_\perp$:

$$\tau_\perp = \tau \sin B = \ln\left[\frac{I_0}{I-b}\right]\sin B. \tag{1}$$

All references to the optical depth in this paper refer to $\tau_\perp$.

We use the method of Albers et al. (2012) to convert an array of observation times to coordinates in the ring plane through knowl-

---

* Corresponding author.
*E-mail address:* morgan.rehnberg@colorado.edu (M.E. Rehnberg).

http://dx.doi.org/10.1016/j.icarus.2017.06.033
0019-1035/

edge of the position and orientation of the planet and spacecraft derived from NAIF SPICE.[1] Longitude in this system is measured prograde from the ascending node of Saturn's equatorial plane on Earth's J2000 equator. We can estimate the uncertainty in the absolute radial coordinate by comparing the computed location of the outer Keeler Gap edge with the location tabulated in French et al. (2017). For the observations used in this study, the 1-$\sigma$ radial uncertainty is 0.76 km. Gap sizes, however, are a relative measurement and not subject to the absolute radial uncertainty.

**Table 1**
Several measures of the radial resolution of the occultations used in this work. See Section 2.2 for an explanation of each measure. All projected stellar radii $r_S$ are computed using distances from Hipparchus (van Leeuwen, 2007).

| Occultation | $r_G$ (m) | $r_S$ (m) | $r_F$ (m) |
|---|---|---|---|
| $\beta$ Lupi R57 | 9.8 | 0.95[a] | 8.4 |
| $\zeta$ Centauri R60 | 9.3 | 1.04[b] | 9.4 |
| $\zeta$ Centauri R62 | 9.1 | 0.81[b] | 8.3 |
| $\epsilon$ Centauri R65 | 10.0 | 1.1[c] | 9.2 |
| $\beta$ Crucis R98 | 6.1 | 1.8[d] | 8.8 |
| $\alpha$ Virginis R134 | 10.1 | 0.63[e] | 5.2 |
| $\alpha$ Virginis R173_out | 8.4 | 1.8[e] | 8.8 |

Stellar radii:
[a] Underhill et al. (1979).
[b] Fitzpatrick and Massa (2005).
[c] Hohle et al. (2010).
[d] Cohen et al. (2008).
[e] Harrington et al. (2009).

### 2.2. Resolution

For a study of such small structures, we must carefully examine the resolution of our observations. The simplest measure of this is the geometric resolution $r_G$, which is the change between where the line of sight from HSP to the occulted star pierces the ring in one integration period to where it does so in the next. This varies by less than a meter in the occultations used in this study and the largest value for each observation is listed in Table 1.

Of course, stars are not truly point sources, so they have a projected diameter on the ring. With a small-angle approximation, we can estimate the projected star diameter $r_S$:

$$r_S = \frac{d_{\text{ring}} D_{\text{star}}}{d_{\text{ring}} + d_{\text{star}}}, \tag{2}$$

where $d_{\text{ring}}$ and $d_{\text{star}}$ are the distance from *Cassini* to the ring and star, respectively, and $D_{\text{star}}$ is the diameter of the star.

We estimate the diffraction limit of our observations as the size of the Fresnel zone, $r_F = \sqrt{\lambda d_{\text{ring}}/2}$, where $\lambda$ is the wavelength of the occulted light. The values listed in Table 1 are computed with $\lambda = 190$ nm, the longest wavelength observed by HSP.

Unless otherwise noted, references to the resolution in this paper are to the geometric resolution. In no observation is the geometric resolution substantially different from the diffraction limit.

### 2.3. Data selection

Occultations are labeled by the star occulted and the *Cassini* revolution during which the observation occurred. In some observations, the track of the occultation through the ring plane moves both inwards and outwards. We treat the ingress and egress as separate occultations and they are labeled with an 'in' or 'out' after the *Cassini* rev. By this standard, HSP has observed more than 200 stellar occultations since the arrival of *Cassini* at Saturn. Because this work examines the rings on their smallest scale, however, we select only observations that match certain requirements.

**Table 2**
An overview of the relevant parameters for the occultations used in this work. All values are averaged across the A ring. The track and viewing angles typically vary less than 1° across the ring.

| Occultation | $I_0\Delta t$ | $B$ (°) | $\phi_{\text{track}}$ (deg) | $\phi_{\text{view}}$ (°) | Gaps |
|---|---|---|---|---|---|
| $\beta$ Lupi R57 | 151.6 | 49.6 | 154.3 | 228.5 | 52,537 |
| $\zeta$ Centauri R60 | 210.0 | 53.6 | 170.6 | 230.1 | 53,061 |
| $\zeta$ Centauri R62 | 213.8 | 53.6 | 9.0 | 67.9 | 70,584 |
| $\epsilon$ Centauri R65 | 262.0 | 59.6 | 172.6 | 228.0 | 49,786 |
| $\beta$ Crucis R98 | 273.9 | 65.2 | 155.8 | 198.4 | 123,911 |
| $\alpha$ Virginis R134 | 150.8 | 17.3 | 151.8 | 291.0 | 50,428 |
| $\alpha$ Virginis R173_out | 123.2 | 17.3 | 302.3 | 95.4 | 49,510 |

We restrict our dataset to those observations that meet the following criteria in the A ring:

1. Radial resolution $\leq 10$ m
2. $I_0\Delta t > 100$ counts
3. Complete coverage of A ring
4. Not occulting a "visual" double star[2]

Table 2 lists the occultations that meet these criteria and are included in this study. The selected observations span a period of time from 26 January 2008 to 19 October 2012.

### 2.4. Self-gravity wake geometry

We adopt a coordinate system defined by increasing ring-plane radius from Saturn and the direction of orbital motion. All angles are measured in a positive direction from the positive radial axis, as depicted in Fig. 1. Due to the motion of *Cassini*, in each successive integration period the point at which the occultation pierces the rings falls on a different location. We call the track angle $\phi_{\text{track}}$ the instantaneous angle at which this point is moving. We call the viewing angle $\phi_{\text{view}}$ the instantaneous angle made between the positive radial direction and the vector from the spacecraft to the occulted star, projected onto the ring plane. The pitch angle $\phi_{\text{wake}}$ is the angle at which the self-gravity wake structures are canted. Our pitch angle is defined differently than in other works:

$$\phi_{\text{wake}} = 180^\circ - \phi_{\text{Colwell, Hedman}} = 90^\circ + \phi_{\text{Salo}}. \tag{3}$$

See Section 3 of Hedman et al. (2007) and Fig. 6 of Salo et al. (2004) for their definitions.

Although we make our measurements in $dr$, through knowledge of the pitch and track angles, these can be converted to the true gap width $S$. Since $\phi_{\text{wake}} > 90^\circ$,

$$S = dr\left|\frac{\sin(\phi_{\text{wake}} - \phi_{\text{track}})}{\cos\phi_{\text{track}}}\right|. \tag{4}$$

Note that $S$ has a pole where an occultation changes radial direction ($\phi_{\text{track}} = 90^\circ, 270^\circ$).

## 3. Methods

We employ a variation of the $m$-test algorithm developed for the Uranian rings by Colwell et al. (1990) and used subsequently to investigate clumping in Saturn's F ring (Esposito et al., 2008; Meinke et al., 2012). This technique searches for consecutive series of highly statistically-unlikely data points within a given observation. Our modified version, described below, searches for tenuous regions rather than dense ones and applies more stringent constraints.

---

[1] Geometry specific to stellar occultations was computed with code provided by M. Sremčević.

[2] $\beta$ Centauri, $\beta$ Crucis, and $\alpha$ Virginis are spectroscopic binaries, but this has no bearing on a HSP occultation.